TABLE 4
Potential Radiation Exposures to the Public from Four Men with Skeletal Metastases from Prostate Cancer Treated with Rhenium-188-(Sn)HEDP

Time postinjection	Radiation exposures (mean ± 1 s.d.) in mR/hr/10 mCi*	
	Distance from the patient axis	
	46 cm	1 m
0 hr	0.77 ± 0.22	0.24 ± 0.07
4 hr	0.42 ± 0.25	0.17 ± 0.08
24 hr	0.08 ± 0.06	<0.06

*1 mR/hr/10 mCi = 7×10^{-10} coul/kg/hr/MBq.

yields and purity of ^{188}Re(Sn)HEDP may be obtained using ^{188}Re from neutron irradiation in a nuclear reactor of either enriched ^{187}Re or naturally occurring rhenium targets or from perrhenate obtained from a ^{188}W/^{188}Re generator system. The generator would have the advantages of onsite availability in large cancer centers or in countries where nuclear reactors are not readily accessible. The use of naturally occurring rhenium targets would eliminate the cost of obtaining enriched target material but would require therapy with a combination of ^{188}Re and ^{186}Re(Sn)HEDP, both of which may be useful agents.

The biodistribution and radiation dosimetry of ^{188}Re(Sn)HEDP are quite similar to those found with ^{186}Re(Sn)HEDP, and the limited data in this study suggest similar benefits and toxicities of the two compounds. Moreover, the short physical half-life of ^{188}Re combined with the rapid renal clearance of HEDP results in such low potential radiation exposures to other people from patients treated with ^{188}Re(Sn)HEDP that same-day outpatient therapy may be feasible.

These considerations indicate an appealing flexibility in the production and use of ^{188}Re(Sn)HEDP for treatment of skeletal metastases that warrant further investigation.

ACKNOWLEDGMENTS

This work was supported by the National Cancer Institute, National Institutes of Health Grant CA-32863, by a grant from the Department of Energy for the production of ^{188}Re by the University of Missouri Research Reactor Facility and by NeoRx Corp., Seattle, WA, which prepared the material used in the targets for ^{188}Re production.

REFERENCES

1. Hosain F, Spencer RP. Radiopharmaceuticals for palliation of metastatic osseous lesions. Biologic and physical background. *Semin Nucl Med* 1992;22:11–16.
2. Maxon HR, Schroder LE, Thomas SR, et al. Rhenium-186-(Sn)HEDP for treatment of painful osseous metastases: initial clinical experience in 20 patients with hormone-resistant prostate cancer. *Radiology* 1990;176:155–159.
3. Callahan AP, Rice DE, Knapp FF Jr. Rhenium-188 for therapeutic applications from an alumina-based tungsten-188/rhenium-188 radionuclide generator. *NucCompact-Eur/Am Commun Nucl Med* 1989;20:3–6.
4. Maxon HR, Deutsch EA, Thomas SR, et al. Rhenium-186(Sn)HEDP for treatment of multiple metastatic foci in bone: human biodistribution and dosimetric studies. *Radiology* 1988;166:501–507.
5. Maxon HR, Schroder LE, Hertzberg VS, et al. Rhenium-186(Sn)HEDP for treatment of painful osseous metastases: results of a double-blind crossover comparison with placebo. *J Nucl Med* 1991;32:1877–1881.

Biodistribution Studies on L-3-[Fluorine-18]Fluoro-α-Methyl Tyrosine: A Potential Tumor-Detecting Agent

Tomio Inoue, Katsumi Tomiyoshi, Tetsuya Higuichi, Khalil Ahmed, Muhammad Sarwar, Keiko Aoyagi, Shigeko Amano, Saleh Alyafei, Hong Zhang and Keigo Endo

Department of Nuclear Medicine, Gunma University School of Medicine, Gunma, Japan

Iodine-123-α-methyl tyrosine has proven to be a promising SPECT agent for imaging amino acid uptake in tumors. We developed L-[3-^{18}F]-α-methyl tyrosine (FMT) for PET studies. The aim of this study was to investigate its potential use as a tumor-detecting agent by using tumor-bearing mice. **Methods:** We investigated the biodistribution in normal BALB/C mice and BALB/cA nude mice bearing human rectal cancer cell line (LS180) until 120 min postinjection. FMT tumor uptake at 60 min postinjection in mice with LS180 rectal cancer, RPMI1788 B-cell lymphoma and MCF7 mammary cell carcinoma was assessed, and the results were compared with ^{18}F-fluoro-2-deoxy-D-glucose (FDG) tumor uptake. The effect of competitive inhibition of large neutral amino acid transport system using unlabeled L-alanine was also investigated. **Results:** The amount of FMT in blood fell to 1.05%ID/20 g at 60 min postinjection, whereas that in the pancreas was 15.2%ID/20 g, resulting in a high pancreas-to-blood ratio of 14.5. In other organs, initial uptake peaked at 5 min postinjection and then declined with time. In LS180 tumor-bearing mice, peak FMT uptake in tumor was observed at 60 min postinjection. Tumor-to-blood and tumor-to-muscle ratios ranged from 1.60 to 2.94 and from 2.79 to 3.25 over the 120-min observation period. Tumor uptake of FMT was clearly reduced by inhibition of the amino acid transport system. In mice with LS180 and MCF7 tumors, FMT tumor uptake at 60 min postinjection was significantly higher than FDG tumor uptake, whereas in RPMI1788 lymphoma, uptake of FDG was significantly higher than FMT tumor uptake. Tumor-to-blood ratios of FMT in mice with LS180, RPMI1788 and MCF7 tumor at 60 min postinjection were 1.82, 5.88 and 3.56, respectively. **Conclusion:** FMT, like other fluorinated amino acids, may become a promising tumor-detecting agent for PET, assuming that efficient methods of radiosynthesis are developed.

Key words: fluorine-18-methyl tyrosine; biodistribution studies; PET

J Nucl Med 1998; 39:663–667

A glucose analog, ^{18}F-2-fluoro-2-deoxy-D-glucose (FDG), has been widely used for tumor imaging with PET, and its usefulness for detecting various malignant tumors, such as

Received Mar. 1., 1997; revision accepted Jun. 12, 1997.

For correspondence or reprints contact: Tomio Inoue, MD, Department of Nuclear Medicine, Gunma University School of Medicine, 3-39-22 Showa-machi Maebashi, Gunma 371, Japan.

malignant lymphoma (*1*), lung cancer (*2*), breast cancer (*3*) and colorectal cancer (*4*), has been reported by many investigators. Experimental studies have demonstrated that FDG accumulates in macrophages and granulation tissue, as well as in cancer cells (*5*). Also, an essential amino acid tracer, L-[methyl-^{14}C]methionine (^{14}C-Met), accumulates more specifically in viable cancer cells (*6*). L-[methyl-^{11}C]methionine (^{11}C-Met) for PET tumor imaging has also proven to be useful in delineating brain tumors (*7*), detecting lung cancer (*8*) and evaluating treatment response of malignant tumors (*9*). However, the short half-life (20 min) of ^{11}C requires in-house radiosynthesis and repeated radiolabeling for each PET study, resulting in a limited number of PET studies. Furthermore, methionine has too many metabolic pathways to obtain rate constants by using kinetic models (*10–12*). To overcome these drawbacks of ^{11}C-Met, an amino acid tracer with a long half-life of ^{18}F is desirable for PET tumor imaging. From this viewpoint, L-[2-^{18}F]fluorotyrosine (^{18}F-Tyr) (*13,14*), L-[2-^{18}F]fluorophenylalanine (^{18}F-Phe) (*15*) and ^{123}I-L-α-methyl tyrosine (IMT) (*16–18*) have been developed and evaluated as tumor-detecting agents. However, the use of ^{18}F-Tyr and ^{18}F-Phe remains limited because of rather ineffective radiosynthesis. A clinical application similar to FDG appears to be difficult at this time. L-[3-^{18}F]-α-methyl tyrosine (FMT) was selected as a tumor-detecting amino acid tracer for PET imaging (*19*). In this study, we investigated the potential use of FMT as a tumor-detecting agent for PET imaging by using experimental tumor models.

MATERIALS AND METHODS

The code of ethics for the use of animals in this study was approved by the Cyclotron Center Committee of Gunma University School of Medicine.

Preparation of FMT

FMT was synthesized according to the method of Tomiyoshi et al. (*19*). Briefly, L-α-methyltyrosine was fluorinated by [^{18}F]acetylhypofluoride, and the separation and purification of FMT were performed by a remote control system.

The mean radiochemical yield of FMT was 10%, with respect to the [^{18}F]F_2 production, and the radiochemical purity ranged from 96% to 99%. The specific activity of FMT was > 0.12 TBq/mmol, and the injected dose of cold substrate, L-α-methyltyrosine, in the solution was approximately 5 μg/kg mouse body weight, comparable to a dose of less than $1/(1 \times 10^6)$ of the LD_{50} of DL-m-fluoro-α-methyltyrosine (*20*) and a dose of less than 1/1000 of the therapeutic dose of L-α-methyltyrosine (*21*).

FMT Distribution in Tissue of Normal Mice

Seven-week-old female BALB/C mice (18–22 g), bred and maintained in a specific pathogen-free mouse colony, were used. Mice were injected intravenously into the tail vein with 370 kBq of FMT in 0.1 ml of saline. Blood samples were taken at 5, 30, 60 and 120 min after FMT injection. Mice were killed immediately after blood samples were taken. Tissues of interest were dissected out, weighed and counted for ^{18}F radioactivity. Uptake of FMT was expressed as the percentage of injected dose per gram (%ID/g) of tissue or blood and normalized to an average weight of 20 g using the following formula:

$$\%ID/g(\%ID/20g) = \frac{\text{cpm tissue/tissue weight in g}}{\text{cpm ID/animal weight in g}} \times \frac{\text{animal weight in g}}{20} \times 100.$$

FMT Distribution in Tumor-Bearing Mice

Four-week-old female BALB/cA Jcl-nu nude mice were transplanted with 10^5 LS180 human colorectal cancer cells subcutaneously in the flank. Tracer experiments were conducted about 10 days after the inoculation, when tumors grew to about 10 mm in diameter. Twenty-five mice (18–22 g) were injected intravenously with 370 kBq of FMT to assess the biodistribution at 30, 60 and 120 min postinjection. Uptake of FMT in tissue or blood was expressed as %ID/20 g.

Comparative Study of FMT and FDG Tumor Uptake

The animals studied in this experiment were female BALB/cA nude mice bearing LS180 human colorectal cancer, female severe combined immunodeficiency mice bearing RPMI1788 human B-cell lymphoma and female athymic NCr *nu/nu* mice bearing MCF7 human breast cancer. Five-week-old severe combined immunodeficiency mice, CB 17 *scid/scid*, were transplanted with a suspension of 10^7 RPMI1788 B-cell lymphoma cells injected subcutaneously in the thigh region, and 5-wk-old athymic NCr *nu/nu* mice were transplanted with a suspension of 2×10^6 MCF7 human breast cancer cells injected into the back. A 60-day-release pellet containing 17β-estradiol was implanted subcutaneously in each animal to grow the MCF7 tumors. The growth of MCF7 tumors was stimulated by estradiol to reach 10 mm in diameter 25 days after the inoculation. Biodistribution of FMT or FDG was determined and tumor-to-blood (T/B) and tumor-to-muscle (T/M) ratios of FMT uptake were compared with those of FDG uptake.

Competition with L-Amino Acid

Female BALB/cA Jcl-nu nude mice bearing LS180 colorectal cancer cells were used in this study. Unlabeled L-alanine was used to competitively inhibit FMT uptake via the large neutral amino acid transport system. Five milligrams of L-alanine dissolved in 0.1 ml saline were administered intraperitoneally to mice 30 min prior to FMT injection. Blood samples were taken at 60 min after a 370-kBq FMT injection. Biodistribution of FMT was determined by measuring radioactivity in blood, muscle and tumors, and the results were compared with baseline data of FMT uptake at 60 min postinjection.

Tumor Metabolism of FMT

Female BALB/cA Jcl *nu/nu* nude mice with LS180 tumors were killed at 60 min postinjection, and tumor tissues were homogenized by the addition of 1 ml of distilled water and by ultrasonication at 0°C. Proteins were precipitated by addition of trichloroacetic acid and were sedimented by centrifugation. Radioactivity levels in the pellet (acid-precipitable fraction) and supernatant (acid-soluble fraction) were measured. The supernatant was further analyzed using instant thin-layer chromatography (Gelman Science, Ann Arbor, MI) for identifying unchanged FMT.

The precipitates were further divided into four fractions: lipids, RNA, DNA and proteins, as previously reported (*11*).

Statistical Analysis

The nonparametric Mann-Whitney U-test was used to analyze data. A two-tailed p value of less than 0.05 was considered statistically significant.

RESULTS

FMT Distribution in Tissue of Normal Mice

Rapid clearance of FMT from blood and prominent accumulation of FMT in the kidneys and pancreas were observed in normal mice (Table 1). The amount of FMT in blood fell to 1.05%ID/20 g at 60 min postinjection, whereas that in the pancreas was 15.2%ID/20 g, resulting in a high pancreas-to-blood ratio of 14.5. In other organs, initial uptake at 5 min

TABLE 1
Biodistribution of Fluorine-18-α-Methyl Tyrosine in Normal Mice

Organ	Time After intravenous injection			
	5 min	30 min	60 min	120 min
Blood	6.54 ± 1.36	1.79 ± 0.58	1.05 ± 0.22	0.73 ± 0.18
Brain	1.48 ± 0.20	1.21 ± 0.42	1.08 ± 0.20	0.83 ± 0.34
Heart	3.01 ± 0.64	1.68 ± 0.22	1.08 ± 0.28	0.79 ± 0.42
Lung	3.36 ± 0.72	1.48 ± 0.16	1.06 ± 0.26	0.67 ± 0.38
Liver	5.29 ± 0.56	1.86 ± 0.70	1.14 ± 0.20	0.78 ± 0.18
Spleen	8.13 ± 3.36	2.53 ± 0.76	1.81 ± 1.10	1.65 ± 0.45
Stomach	3.36 ± 1.10	2.19 ± 0.62	1.81 ± 0.54	1.61 ± 0.89
Pancreas	36.07 ± 9.68	12.02 ± 5.22	15.20 ± 6.62	10.49 ± 4.16
Intestine	4.44 ± 1.50	3.35 ± 0.98	1.43 ± 0.60	1.14 ± 0.67
Kidney	24.90 ± 7.96	24.40 ± 13.00	17.07 ± 3.56	10.21 ± 3.53
Bone	1.85 ± 0.32	1.60 ± 0.28	0.69 ± 0.16	0.92 ± 0.25
Muscle	2.72 ± 0.72	1.67 ± 0.70	1.59 ± 0.18	1.24 ± 0.34

Uptakes are expressed as mean ± s.d. of %ID/g tissue normalized to an average weight of 20 g of four or five mice.

postinjection declined with time. FMT uptake in bone was less than 1.0%ID/20 g at 60 and 120 min postinjection.

FMT and FDG Distribution in Blood, Muscle and Tumor Tissue

In mice with LS180 tumors, peak FMT uptake in tumor was observed at 60 min postinjection. The T/B and T/M ratios ranged from 1.60 to 2.94 and 2.79 to 3.25 over the 120-min observation period, respectively (Table 2).

In mice with LS180 and MCF7 tumors, FMT tumor uptake at 60 min postinjection was significantly higher than FDG tumor uptake ($p < 0.05$ and $p < 0.01$). FDG tumor uptake in mice with RPMI1788 lymphoma was significantly higher than FMT tumor uptake ($p < 0.01$). The T/B ratios of FMT at 60 min postinjection in mice with LS180, RPMI1788 and MCF7 tumors were 1.82, 5.88 and 3.56, and T/M ratios of FMT were 3.25, 5.42 and 2.29, respectively. The T/B ratio of FMT at 60 min postinjection in mice with LS180 was significantly lower than that of FDG ($p < 0.01$), but no significant difference was observed in T/B ratios of mice with RPMI1788 and MCF7 tumors. T/M ratios of FMT in mice with LS180 and MCF7 tumors were significantly higher than those of FDG ($p < 0.05$ and $p < 0.01$, respectively).

Competition with L-Amino Acid

Competitive inhibition of the neutral amino acid transport system was observed after injection of unlabeled L-alanine (Fig. 1). Tumor uptake of FMT at 60 min postinjection was clearly reduced after loading L-alanine compared to baseline data ($p < 0.02$); however, no significant change in blood and muscle uptake was observed. T/B and T/M ratios significantly decreased after loading unlabeled L-alanine compared to baseline conditions ($p < 0.02$).

Tumor Metabolism of FMT

The mean and s.d. of acid-soluble fraction and acid-precipitable fraction were 89.0% ± 1.1% and 11.0% ± 1.1%, respectively ($n = 5$). Instant thin-layer chromatography analysis of the supernatant revealed only one peak corresponding to the unmetabolized FMT. The mean and s.d. of the fraction of lipids, RNA, DNA and protein were 5.9% ± 1.2%, 2.7% ± 0.3%, 1.1% ± 0.4% and 1.2% ± 0.5%, respectively ($n = 5$).

DISCUSSION

Radioiodinated IMT was reported to be a promising tumor-detecting agent for SPECT in patients with brain tumors (*16*) and melanoma (*17,18*). A constant tracer concentration during data collection is a prerequisite for SPECT studies using a rotating gamma camera, and IMT satisfied this condition. However, radioiodinated compounds are not adequately stable because of in vivo deiodination. In addition, new technology such as a gamma camera using a 511-keV collimator or coincidence circuit may facilitate imaging with ^{18}F-labeled compounds. For these reasons, we labeled a SPECT tracer for PET, and fundamental studies of radiofluorinated FMT as a tumor-detecting agent for PET imaging were performed.

The maximum radioactivity of produced FMT in this study

TABLE 2
Biodistribution of Fluorine-18-α-Methyl Tyrosine and FDG in Tumor-Bearing Mice

Tissue	LS 180				RPMI1788		MCF7	
	FMT			FDG, 60 min	FMT, 60 min	FDG, 60 min	FMT, 60 min	FDG, 60 min
	30 min	60 min	120 min					
Tumor (T)	2.62 ± 1.18	3.82 ± 1.59*	1.57 ± 0.59	2.23 ± 0.27	2.38 ± 0.16†	15.67 ± 4.27	2.98 ± 0.83†	0.51 ± 0.07
Blood (B)	2.11 ± 1.53	2.12 ± 1.14†	0.76 ± 0.84	0.41 ± 0.22	0.41 ± 0.04*	4.01 ± 0.69	0.88 ± 0.34†	0.13 ± 0.04
Muscle (M)	1.29 ± 0.62	1.53 ± 0.96*	0.75 ± 0.34	3.21 ± 0.85	0.46 ± 0.11*	2.34 ± 0.49	1.42 ± 0.60	0.85 ± 0.22
Ratio								
T/B	1.60 ± 1.07	1.82 ± 1.26†	2.94 ± 1.30	6.00 ± 1.79	5.88 ± 0.54	4.10 ± 1.86	3.56 ± 0.69	4.12 ± 1.41
T/M	3.02 ± 2.86	3.25 ± 2.91*	2.79 ± 2.06	0.73 ± 0.18	5.42 ± 1.34	6.73 ± 1.57	2.29 ± 0.58†	0.60 ± 0.16

*Significant difference from FDG data, $p < 0.05$.
†Significant difference from FDG data, $p < 0.01$.
Uptakes in tumor, blood and muscle are expressed as mean ± s.d. of %ID/g tissue normalized to an average weight of 20 g of five to nine mice.

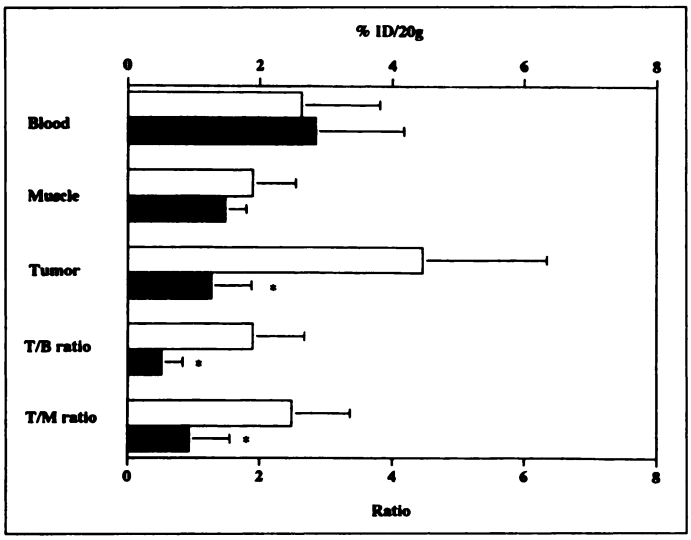

FIGURE 1. Influence on FMT uptake of competitive inhibition with unlabeled L-alanine. Each bar represents the mean ± s.d. of five animals in the baseline group and four animals treated with L-alanine. □ = baseline data; ■ = data after L-alanine loading. * = significant difference at a p value < 0.02. Tumor uptake, T/B ratio and T/M ratio exhibited a significant decrease after L-alanine treatment, whereas blood and muscle uptake showed no significant change.

was 600 MBq, which was half of the FDG produced under the same conditions of bombardment of the cyclotron. A more efficient radiosynthesis of FMT may be required for a clinical application like FDG.

Rapid blood clearance, maximum tissue uptake and prolonged retention in the kidneys and pancreas were found in the tissue biodistribution study of FMT, which seemed to be similar to the biodistribution of an amino acid analog, IMT (*22,23*). Little radioactivity in the bone observed in this study demonstrated in vivo stability of this compound, which suggested the presence of a small amount of free ^{18}F-fluoride by defluorination of FMT. Blood clearance of FMT showed the initial high peak count followed by the slow reduction until 120 min postinjection (Table 1), similar to the blood clearance of IMT, as reported previously (*23*). Unlike natural amino acid, IMT is proven not to be incorporated into proteins (*24*), and our results of FMT metabolism suggested that most of FMT in the tumor at 60 min postinjection was not metabolized and not incorporated into proteins like IMT. Fluorine-18-tyrosine is metabolized and incorporated into the protein (*14*) and its metabolites appeared in blood at 60 min postinjection. This metabolic fate of ^{18}F-Tyr requires a complicated kinetic model for quantitative PET study (*14*). A kinetic model of FMT could be simplified because most of FMT in the tumor is not metabolized like IMT (*25*). It seems to be the advantage of FMT versus the other fluorinated natural amino acids such as ^{18}F-Tyr.

In this study, peak FMT uptake in the tumor was observed at 60 min postinjection, but there was no significant statistical difference among 30-, 60- and 120-min tumor uptakes of FMT. IMT tumor uptake was reported to reach peak level 15 min postinjection and decreased slowly thereafter (*23,24*), probably due to the washout of unmetabolized tracer or the deiodination of ^{123}I from IMT. On the contrary, prolonged retention of FMT in the tumor would be highly desirable for tumor imaging with PET.

FDG is widely used in detecting malignant tumors because of the high accumulation in various tumors and rapid blood clearance to reach the suitable tumor-to-nontumor count ratio as T/B and T/M ratios. We used three varieties of malignant tumors, human colorectal cancer (LS180), malignant lymphoma (RPMI1788) and breast cancer (MCF7), because FDG is proven to be clinically useful in detecting these tumors (*1–4*). In this study, we found that the tumor detectability of FMT was equal to or at times superior to that of FDG. FDG uptake seems to be higher in rapidly growing tumors such as RPMI1788 and LS180 tumors than it is in slow-growing tumors such as MCF7. Although FMT uptake appears to be similar among three different tumors, there is no significant relationship to the tumor growing rate. SPECT with IMT has already been proven to be useful in the detection of tumors, but only in patients with brain tumors (*16,24*) and melanoma (*18*). Our results suggest that PET imaging using FMT is likely to have high detectability of lymphoma, colorectal cancer and breast cancer in humans.

The competition with L-alanine on FMT uptake in the LS180 tumor system was clearly demonstrated (Fig. 1). It is well known that the transport system of a specific amino acid into the brain is inhibited by an infusion of large amounts of other amino acids that use the same carrier system (*26*). It has also been shown for IMT uptake in glioma (*27*) and experimental animal tumors (*23*). This study suggests the accumulation of FMT in tumor cells via an amino acid transport system.

CONCLUSION

The biodistribution of FMT in mice was similar to that of IMT, as reported previously (*22,23*). FMT may accumulate in tumor cells via an amino acid transport system and have high tumor detectability, as does FDG, although further experiments analyzing the metabolites of FMT in tumor may be needed to assess the principal factors that determine tumor uptake. FMT, like other fluorinated amino acids, may become a promising tumor-detecting agent for PET if efficient methods of radiosynthesis are developed.

REFERENCES

1. Okada J, Yoshikawa K, Itami M, et al. Positron emission tomography using fluorine-18-fluorodeoxyglucose in malignant lymphoma: a comparison with proliferative activity. *J Nucl Med* 1992;33:325–329.
2. Gupta NC, Frank AR, Dewan NA, et al. Solitary pulmonary nodules: detection of malignancy with PET with 2-[F-18]-fluoro-2-deoxy-D-glucose. *Radiology* 1992;184: 441–444.
3. Wahl RL, Cody RL, Hutchins GD, Mudgett EE. Primary and metastatic breast carcinoma: initial clinical evaluation with PET with the radiolabeled glucose analog 2-[^{18}F]-fluoro-2-deoxy-D-glucose. *Radiology* 1991;179:765–770.
4. Strauss LG, Conti PS. The applications of PET in clinical oncology. *J Nucl Med* 1991;32:623–648.
5. Kubota R, Kubota K, Yamada S, Tada M, Ido T, Tamahashi N. Microautoradiographic study for the differentiation of intratumoral macrophages, granulation tissues and cancer cells by the dynamics of fluorine-18-fluorodeoxyglucose uptake. *J Nucl Med* 1994;35:104–112.
6. Kubota R, Kubota K, Yamada S, et al. Methionine uptake by tumor tissue: a microautoradiographic comparison with FDG. *J Nucl Med* 1995;36:484–492.
7. Ogawa T, Shishido F, Kanno I, et al. Cerebral glioma: evaluation with methionine PET. *Radiology* 1993;186:45–53.
8. Kubota K, Matsuzawa T, Ito M, et al. Lung tumor imaging by positron emission tomography using C-11 L-methionine. *J Nucl Med* 1985;26:37–42.
9. Kubota K, Matsuzawa T, Takahashi T, et al. Rapid and sensitive response of carbon-11-L-methionine tumor uptake to irradiation. *J Nucl Med* 1989;30:2012–2016.
10. Ishiwata K, Kubota K, Murakami M, et al. Re-evaluation of amino acid PET studies: can the protein synthesis rates in brain and tumor tissues be measured in vivo? *J Nucl Med* 1993;34:1936–1943.
11. Ishiwata K, Kubota K, Murakami M, Kubota R, Senda M. A comparative study on protein incorporation of L-[methyl-^{3}H]methionine, L-[1-^{14}C]leucine and L-2-[^{18}F]fluorotyrosine in tumor-bearing mice. *Nucl Med Biol* 1993;20:895–899.
12. Ishiwata K, Enomoto K, Sasaki T, et al. A feasibility study on L-[^{1}C]tyrosine and L-[Methyl-carbon-11]methionine to assess liver protein synthesis by PET. *J Nucl Med* 1996;37:279–285.
13. Wienhard K, Herholz K, Coenen HH, et al. Increased amino acid transport into brain tumors measured by PET of L-(2-^{18}F)fluorotyrosine. *J Nucl Med* 1991;32:1338–1346.
14. Coenen HH, Kling P, Stöcklin G. Cerebral metabolism of L-[2-^{18}F]fluorotyrosine, a new PET tracer of protein synthesis. *J Nucl Med* 1989;30:1367–1372.
15. Kubota K, Ishiwata K, Kubota R, et al. Feasibility of fluorine-18-fluorophenylalanine for tumor imaging compared with carbon-11-L-methionine. *J Nucl Med* 1996;37:320–325.
16. Biersack HJ, Coenen HH, Stöcklin G, et al. Imaging of brain tumors with L-3-[^{123}I]iodo-α-methyl tyrosine and SPECT. *J Nucl Med* 1989;30:110–112.

17. Bockslaff H, Kloster G, Stöcklin G, Safi N, Bornemann H. Studies on L-3-^{123}Iodo-α-methyl-tyrosine: a new potential melanoma seeking compound. *Nuklearmedizin* 1980;(suppl 17):179–182.
18. Bockslaff H, Kloster G, Dausch D, Schad K, Hundeshagen H, Stöcklin G. First clinical results using L-3-^{123}I-α-methyltyrosine for the non-invasive detection of intraocular melanomas. *Nuklearmedizin* 1981;(suppl 18):840–844.
19. Tomiyoshi K, Ahmed K, Muhammad S, et al. Synthesis of isomers of ^{18}F-labeled amino acid radiopharmaceutical: position 2- and 3-L-^{18}F-α-methyl tyrosine using a separation and purification system. *Nucl Med Commun* 1997;18:169–175.
20. Neissman A, Koe BK. m-Fluorotyrosine convulsions and mortality: relationship to catecholamine and citrate metabolism. *J Pharmacol Exp Ther* 1967;155:135–144.
21. Engelman K, Horwitz D, Jéquier E, Sjoerdsma A. Biochemical and pharmacologic effects of α-methyltyrosine in man. *J Clin Invest* 1968;47:577–594.
22. Tisljar U, Kloster G, Ritzl F, Stöcklin G. Accumulation of radioiodinated L-α-methyltyrosine in pancreas of mice: concise communication. *J Nucl Med* 1979;20:973–976.
23. Deehan B, Carnochan P, Trivedi M, Tombs A. Uptake and distribution of L-3-[I-125] iodo-α-methyl tyrosine in experimental rat tumors: comparison with blood flow and growth rate. *Eur J Nucl Med* 1993;20:101–106.
24. Langen KJ, Coenen HH, Roosen N, et al. SPECT studies of brain tumors with L-3-[^{123}I]iodo-α-methyl tyrosine: comparison with PET, ^{124}IMT and first clinical results. *J Nucl Med* 1990;31:281–286.
25. Kawai K, Fujibayashi Y, Yonekura Y, et al. Canine SPECT studies for cerebral amino acid transport by means of ^{123}I-3-iodo-α-methyl tyrosine and preliminary kinetic analysis. *Ann Nucl Med* 1995;9:47–50.
26. Pardrige WM. Kinetics of competitive inhibition of neutral amino acid transport across the blood-brain barrier. *J Neurochem* 1977;28:103–108.
27. Langen KJ, Roosen N, Coenen HH, et al. Brain and brain tumor uptake of L-3-[^{123}I]iodo-α-methyl tyrosine: competition with natural L-amino acids. *J Nucl Med* 1991;32:1225–1228.

Effects of Radiolysis on Yttrium-90-Labeled Lym-1 Antibody Preparations

Q.A. Salako, R.T. O'Donnell and S.J. DeNardo
Department of Internal Medicine, Molecular Cancer Institute, University of California, Davis, Sacramento, California

The physical half-life of 2.6 days and 2.2 MeV beta emissions of ^{90}Y provide excellent properties for radioimmunotherapy applications. However, the clinically useful beta particles may be a source of radiation-induced damage of ^{90}Y-labeled immunoconjugate radiopharmaceuticals during preparation or short-term storage. The stability of ^{90}Y-labeled Lym-1 antibody was studied in standard radiopharmacy conditions to establish a formulation at which radiolysis is not a problem. **Methods:** Lym-1–2IT-BAD immunoconjugate intermediate was prepared according to our standard procedure, then labeled with ^{90}Y at 1, 2, 4 and 9.4 mCi/mg Lym-1 using 0.5 *M* tetramethylammonium acetate, pH 7, labeling buffer. Each mixture was challenged in diethylenetriaminepentaacetic acid to remove nonspecifically bound ^{90}Y. The ^{90}Y-2IT-BAD-Lym-1 products were purified by centrifuged molecular sieving column chromatography. The radiochemical purity and immunoreactivity of each preparation was monitored daily by high-performance liquid chromatography (HPLC) and solid-phase radioimmunoassay, respectively, for 3 days. The preparation at 2 mCi/mg was also formulated in 4% (wt/vol) human serum albumin (HSA) overall and at 9.4 mCi/mg in five-fold water, 4 and 10% (wt/vol) HSA overall; all were monitored as above. **Results:** The monomeric quality and purity profile of products at 1 and 2 mCi/mg were retained (≥ 80%) as was their immunoreactivity (≥ 75%) over 3 days. The radiochemical purity and immunoreactivity of the product at 4 mCi/mg declined to 65% and 28%, respectively, by 3 days after preparation and in just 48 hr, the product at 9.4 mCi/mg had degraded to 21% in radiochemical purity with only 3% immunoreactivity. The current HPLC data and earlier published chromatographic evidence did not support a compromised radiochemical integrity of ^{90}Y-DOTA complexes by loss of ^{90}Y from the DOTA chelate. **Conclusion:** Radiolysis of ^{90}Y-labeled antibody preparations did not appear to be a problem at ^{90}Y-2IT-BAD-Lym-1 products ≤ 2 mCi/mg. Human serum albumin proved to be an effective radioprotectant as the initial 100% immunoreactivity of the product at 2 mCi/mg was retained for 72 hr. The results underscore the need for appropriate formulations and dilutions of clinical doses of ^{90}Y immunopharmaceuticals immediately after manufacture.

Key Words: yttrium-90; antibody; radiolysis; radioprotectant

J Nucl Med 1998; 39:667–670

Received Apr. 14, 1997; revision accepted Jul. 16, 1997.
For correspondence contact: Qansy Salako, PhD, Molecular Cancer Institute, 1508 Alhambra Blvd., Sacramento, CA 95816.

The lethal effect of energetic beta particles from ^{90}Y on tumor cells is fundamental to its use in radioimmunotherapy (RIT). The development of better methods for delivery of ^{90}Y beta particles to tumor cells has continued to attract research interest. This research has included the development of polylactic acid microspheres as carriers for the ionic ^{90}Y matrix (*1*), ^{90}Y-Al-Si oxide glasses (*2*) and the antibody-based ^{90}Y radioimmunoconjugates (*3*). In each of these procedures, the stability of the yttrium preparations, both in vitro and in vivo, is crucial for successful ^{90}Y radionuclide therapy. While several articles are available on diminished efficacy of ^{90}Y radioimmunoconjugates due to ionization of the radiometal from the chelates (*4*), transchelation to proteins (*5*) or radiometal trapping in normal cell lysosomes (*6,7*), articles on radiation damage to the peptide or protein substrates (radiolysis) are scarce.

Encouraging results in clinical therapy protocols involving ^{90}Y-labeled monoclonal antibody (MAb) preparations (*8–10*) may lead to an increase in the use of ^{90}Y radiopharmaceuticals and their injected doses (mCi). Therefore, ^{90}Y radiochemistry has become more efficient by using methods involving minimal MAb, high radioactivity yields and optimum specific activity of final products. At high specific activity, however, ^{90}Y immunoconjugates are particularly prone to radiolysis due to the energetic particulate emissions from yttrium.

For our current clinical RIT protocols, several ^{90}Y-MAb conjugates were prepared. We investigated evidence of radiolysis over time in ^{90}Y-labeled 2IT-BAD-Lym-1 conjugate at varying specific activities. The extent of radiolysis on this immunoconjugate was compared, when formulated with or without human serum albumin (HSA), as a possible radioprotectant.

MATERIALS AND METHODS

Lym-1 (Techniclone, Inc., Tustin, CA) is a murine IgG2a MAb specific for membrane antigens found on malignant cells of most patients with B-cell lymphoma (*11*). Yttrium-90 was purchased as a concentrated carrier-free radiochemical grade $^{90}YCl_3$ in 0.05M HCl from Battelle-PNNL Laboratory (Richland, WA). Diethylenetriaminepentaacetic acid (DTPA) was obtained from Fisher Scien-